Paper 223

©Civil-Comp Press, 2012
Proceedings of the Eleventh International Conference
on Computational Structures Technology,
B.H.V. Topping, (Editor),
Civil-Comp Press, Stirlingshire, Scotland

Buckling of Laminated and Functionally Graded Plates using Radial Basis Functions

A.M.A. Neves[1], A.J.M. Ferreira[1], E. Carrera[3], M. Cinefra[3]
C.M.C. Roque[2], C.M. Mota Soares[4] and R.M.N. Jorge[1]
[1] Departamento de Engenharia Mecânica, [2] INEGI
Faculdade de Engenharia, Universidade do Porto, Portugal
[3] Departament of Aeronautics and Aerospace Engineering
Politecnico di Torino, Italy
[4] Instituto Superior Técnico, Lisbon, Portugal

Abstract

A hyperbolic sine shear deformation theory is used for the buckling analysis of functionally graded plates, accounting for through-the-thickness deformations. The linearized buckling equations and boundary conditions are derived using Carrera's Unified Formulation and further interpolated by collocation with radial basis functions. Numerical results demonstrate the accuracy of the present approach.

Keywords: plates and shells, collocation, meshless methods, functionally graded plates.

1 Introduction

A conventional functionally graded plate (FGM) considers a continuous variation of material properties over the thickness direction by mixing two different materials [1]. The material properties of the FGM plate are assumed to change continuously throughout the thickness of the plate, according to the volume fraction of the constituent materials. Analysis of vibrations of FGM plates can be found in Batra and Jin [2], Ferreira et al. [3], Vel and Batra [4], Zenkour [5], and Cheng and Batra [6]. The analysis of mechanical buckling of FGM structures is less common in the literature. It can be found in Najafizadeh and Eslami [7], Zenkour [5], Cheng and Batra [6], Birman [8], Javaheri and Eslami [9].

Typically, the analysis of FGM plates is performed using the clasical plate theory (CPT) [10, 11], the first-order shear deformation theory (FSDT) [12, 2, 3, 13] or higher-order shear deformation theories (HSDT) [14, 15, 3, 16, 13]. The FSDT gives acceptable results but depends on the shear correction factor which is hard to find as it depends on many parameters. There is no need of a shear correction factor when using a HSDT but linearized buckling equations are more complicated than those of the FSDT. The Unified Formulation proposed by Carrera [17, 18] made the implementation of such theories easier.

The use of alternative-to-Finite element methods for the analysis of plates, such as the meshless methods based on collocation with radial basis functions is atractive due to the absence of a mesh and the ease of collocation methods. In recent years, radial basis functions (RBFs) showed excellent accuracy in the interpolation of data and functions. Kansa [19] introduced the concept of solving partial differential equations by an unsymmetric RBF collocation method based upon the multiquadric interpolation functions. The authors have applied successfully the RBF collocation technique to the static and dynamic analysis of composite structures [20, 21, 22, 23, 24, 25, 26, 27, 28, 29]. The present paper considers the thickness stretching issue on the buckling analysis of FGM plates, by a meshless technique based on collocation with radial basis functions.

2 Problem formulation

The problem consists of a rectangular sandwich plate of plan-form dimensions a and b and uniform thickness h. The co-ordinate system is taken such that the x-y plane coincides with the midplane of the plate ($z \in [-h/2, h/2]$). The sandwich core is a ceramic material and skins are composed of a functionally graded material across the thickness direction. The bottom skin varies from a metal-rich surface ($z = h_0 = -h/2$) to a ceramic-rich surface while the top skin face varies from a ceramic-rich surface to a metal-rich surface ($z = h_3 = h/2$) as illustrated in figure 1. The volume fraction of the ceramic phase is obtained from a simple rule of mixtures as:

$$
\begin{aligned}
&V_c = \left(\frac{z - h_0}{h_1 - h_0}\right)^p, \quad z \in [h_0, h_1] \\
&V_c = 1, \quad z \in [h_1, h_2] \\
&V_c = \left(\frac{z - h_3}{h_2 - h_3}\right)^p, \quad z \in [h_2, h_3]
\end{aligned}
\tag{1}
$$

where p is a scalar parameter that allows the user to define the gradation of material properties across the thickness direction of the skins. With this formulation the interfaces between core and skins disappear. Note that the core of the present sandwich and any isotropic material can be obtained as a particular case of the power-law function by setting $p = 0$. The volume fraction for the metal phase is given as $V_m = 1 - V_c$. The sandwich may be symmetric or non-symmetric about the mid-plane as we may vary the thickness of each face. Figure 2 shows a non-symmetric sandwich with volume fraction defined by the power-law (1) for various exponents p, in which top skin thickness is the same as the core thickness and the bottom skin thickness is twice the core thickness. Such thickness relation is denoted as 2-1-1. A bottom-core-top notation is used. 1-1-1 means that skins and core have the same thickness.

The sandwich plate is subjected to compressive in-plane forces acting on the mid-plane of the plate. $\bar{N}_{xx}$ and $\bar{N}_{yy}$ denote the in-plane loads perpendicular to the edges

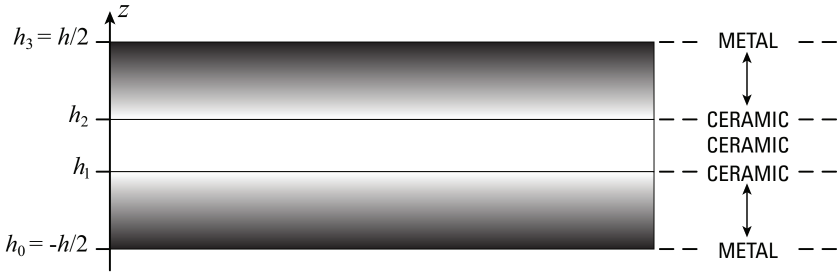

Figure 1: Sandwich with isotropic core and FGM skins.

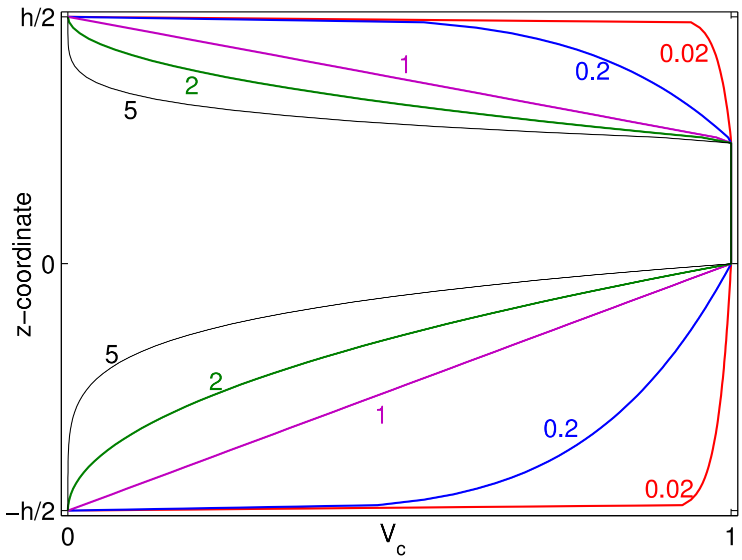

Figure 2: Illustration of a 2-1-1 sandwich with FGM skins for several volume fractions.

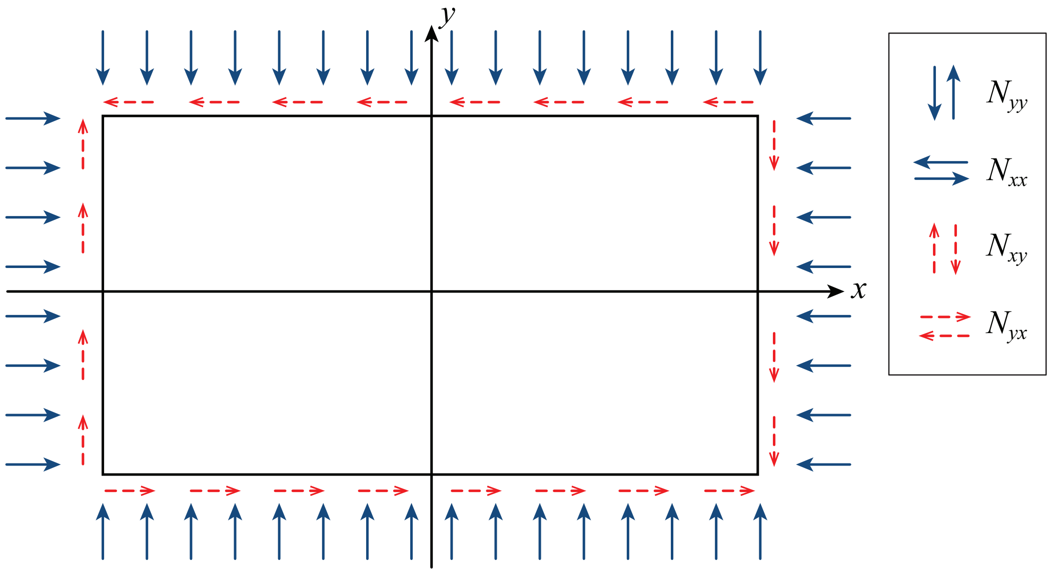

Figure 3: Rectangular plate subjected to in-plane forces.

$x = 0$ and $y = 0$ respectively, and $\bar{N}_{xy}$ denotes the distributed shear force parallel to the edges $x = 0$ and $y = 0$ respectively (see fig. 3).

3 A quasi-3D hyperbolic sine plate shear deformation theory

3.1 Displacement field

The present theory is based on the following displacement field:

$$u(x, y, z, t) = u_0(x, y, t) + zu_1(x, y, t) + \sinh\left(\frac{\pi z}{h}\right) u_Z(x, y, t) \tag{2}$$

$$v(x, y, z, t) = v_0(x, y, t) + zv_1(x, y, t) + \sinh\left(\frac{\pi z}{h}\right) v_Z(x, y, t) \tag{3}$$

$$w(x, y, z, t) = w_0(x, y, t) + zw_1(x, y, t) + z^2 w_2(x, y, t) \tag{4}$$

where u, v, and w are the displacements in the $x-$, $y-$, and $z-$ directions, respectively. u_0, u_1, u_Z, v_0, v_1, v_Z, w_0, w_1, and w_2 are the unknowns to be determined. A constant term is assumed for the transverse displacement component instead of (4) ($w = w_0$) to investigate the effect of the thickness stretching on the buckling load.

3.2 Strains

The strains can be related to the displacement field as:

$$\left\{\begin{array}{c}\epsilon_{xx}\\ \epsilon_{yy}\\ \gamma_{xy}\end{array}\right\}=\left\{\begin{array}{c}\frac{\partial u}{\partial x}+\frac{1}{2}\left(\frac{\partial w_0}{\partial x}\right)^2\\ \frac{\partial v}{\partial y}+\frac{1}{2}\left(\frac{\partial w_0}{\partial y}\right)^2\\ \frac{\partial u}{\partial y}+\frac{\partial v}{\partial x}+\frac{\partial w_0}{\partial x}\frac{\partial w_0}{\partial y}\end{array}\right\},\quad \left\{\begin{array}{c}\gamma_{xz}\\ \gamma_{yz}\\ \epsilon_{zz}\end{array}\right\}=\left\{\begin{array}{c}\frac{\partial u}{\partial z}+\frac{\partial w}{\partial x}\\ \frac{\partial v}{\partial z}+\frac{\partial w}{\partial y}\\ \frac{\partial w}{\partial z}\end{array}\right\} \tag{5}$$

By substitution of the displacement field in (5), the strains are obtained:

$$\left\{\begin{array}{c}\epsilon_{xx}\\ \epsilon_{yy}\\ \gamma_{xy}\end{array}\right\}=\left\{\begin{array}{c}\epsilon_{xx}^{(0)}\\ \epsilon_{yy}^{(0)}\\ \gamma_{xy}^{(0)}\end{array}\right\}+\left\{\begin{array}{c}\epsilon_{xx}^{(nl)}\\ \epsilon_{yy}^{(nl)}\\ \gamma_{xy}^{(nl)}\end{array}\right\}+z\left\{\begin{array}{c}\epsilon_{xx}^{(1)}\\ \epsilon_{yy}^{(1)}\\ \gamma_{xy}^{(1)}\end{array}\right\}+\sinh\left(\frac{\pi z}{h}\right)\left\{\begin{array}{c}\epsilon_{xx}^{(Z)}\\ \epsilon_{yy}^{(Z)}\\ \gamma_{xy}^{(Z)}\end{array}\right\} \tag{6}$$

$$\left\{\begin{array}{c}\gamma_{xz}\\ \gamma_{yz}\\ \epsilon_{zz}\end{array}\right\}=\left\{\begin{array}{c}\gamma_{xz}^{(0)}\\ \gamma_{yz}^{(0)}\\ \epsilon_{zz}^{(0)}\end{array}\right\}+z\left\{\begin{array}{c}\gamma_{xz}^{(1)}\\ \gamma_{yz}^{(1)}\\ \epsilon_{zz}^{(1)}\end{array}\right\}+z^2\left\{\begin{array}{c}\gamma_{xz}^{(2)}\\ \gamma_{yz}^{(2)}\\ \epsilon_{zz}^{(2)}\end{array}\right\}+\frac{\pi}{h}\cosh\left(\frac{\pi z}{h}\right)\left\{\begin{array}{c}\gamma_{xz}^{(Z)}\\ \gamma_{yz}^{(Z)}\\ \epsilon_{zz}^{(Z)}\end{array}\right\} \tag{7}$$

being the strain components obtained as

$$\left\{\begin{array}{c}\epsilon_{xx}^{(0)}\\ \epsilon_{yy}^{(0)}\\ \gamma_{xy}^{(0)}\end{array}\right\}=\left\{\begin{array}{c}\frac{\partial u_0}{\partial x}\\ \frac{\partial v_0}{\partial y}\\ \frac{\partial u_0}{\partial y}+\frac{\partial v_0}{\partial x}\end{array}\right\};\quad \left\{\begin{array}{c}\epsilon_{xx}^{(nl)}\\ \epsilon_{yy}^{(nl)}\\ \gamma_{xy}^{(nl)}\end{array}\right\}=\left\{\begin{array}{c}\frac{1}{2}\left(\frac{\partial w_0}{\partial x}\right)^2\\ \frac{1}{2}\left(\frac{\partial w_0}{\partial y}\right)^2\\ \frac{\partial w_0}{\partial x}\frac{\partial w_0}{\partial y}\end{array}\right\} \tag{8}$$

$$\left\{\begin{array}{c}\epsilon_{xx}^{(1)}\\ \epsilon_{yy}^{(1)}\\ \gamma_{xy}^{(1)}\end{array}\right\}=\left\{\begin{array}{c}\frac{\partial u_1}{\partial x}\\ \frac{\partial v_1}{\partial y}\\ \frac{\partial u_1}{\partial y}+\frac{\partial v_1}{\partial x}\end{array}\right\};\quad \left\{\begin{array}{c}\epsilon_{xx}^{(Z)}\\ \epsilon_{yy}^{(Z)}\\ \gamma_{xy}^{(Z)}\end{array}\right\}=\left\{\begin{array}{c}\frac{\partial u_Z}{\partial x}\\ \frac{\partial v_Z}{\partial y}\\ \frac{\partial u_Z}{\partial y}+\frac{\partial v_Z}{\partial x}\end{array}\right\} \tag{9}$$

$$\left\{\begin{array}{c}\gamma_{xz}^{(0)}\\ \gamma_{yz}^{(0)}\\ \epsilon_{zz}^{(0)}\end{array}\right\}=\left\{\begin{array}{c}u_1+\frac{\partial w_0}{\partial x}\\ v_1+\frac{\partial w_0}{\partial y}\\ w_1\end{array}\right\};\quad \left\{\begin{array}{c}\gamma_{xz}^{(1)}\\ \gamma_{yz}^{(1)}\\ \epsilon_{zz}^{(1)}\end{array}\right\}=\left\{\begin{array}{c}\frac{\partial w_1}{\partial x}\\ \frac{\partial w_1}{\partial y}\\ 2w_2\end{array}\right\} \tag{10}$$

$$\left\{\begin{array}{c}\gamma_{xz}^{(2)}\\ \gamma_{yz}^{(2)}\\ \epsilon_{zz}^{(2)}\end{array}\right\}=\left\{\begin{array}{c}\frac{\partial w_2}{\partial x}\\ \frac{\partial w_2}{\partial y}\\ 0\end{array}\right\};\quad \left\{\begin{array}{c}\gamma_{xz}^{(Z)}\\ \gamma_{yz}^{(Z)}\\ \epsilon_{zz}^{(Z)}\end{array}\right\}=\left\{\begin{array}{c}u_Z\\ v_Z\\ 0\end{array}\right\} \tag{11}$$

where $\epsilon_{\alpha\beta}^{(nl)}$ are the non-linear terms that will originate the linearized buckling equations.

3.3 Elastic stress-strain relations

In the case of isotropic functionally graded materials, the 3D constitutive equations can be written as:

$$
\begin{aligned}
&\left\{\begin{array}{c}\sigma_{xx}\\ \sigma_{yy}\\ \tau_{xy}\end{array}\right\}=\left[\begin{array}{ccc}C_{11}&C_{12}&0\\ C_{12}&C_{11}&0\\ 0&0&C_{44}\end{array}\right]\left\{\begin{array}{c}\epsilon_{xx}\\ \epsilon_{yy}\\ \gamma_{xy}\end{array}\right\}+\left[\begin{array}{ccc}0&0&C_{12}\\ 0&0&C_{12}\\ 0&0&0\end{array}\right]\left\{\begin{array}{c}\gamma_{xz}\\ \gamma_{yz}\\ \epsilon_{zz}\end{array}\right\}\\
&\left\{\begin{array}{c}\tau_{xz}\\ \tau_{yz}\\ \sigma_{zz}\end{array}\right\}=\left[\begin{array}{ccc}0&0&0\\ 0&0&0\\ C_{12}&C_{12}&0\end{array}\right]\left\{\begin{array}{c}\epsilon_{xx}\\ \epsilon_{yy}\\ \gamma_{xy}\end{array}\right\}+\left[\begin{array}{ccc}C_{44}&0&0\\ 0&C_{44}&0\\ 0&0&C_{33}\end{array}\right]\left\{\begin{array}{c}\gamma_{xz}\\ \gamma_{yz}\\ \epsilon_{zz}\end{array}\right\}
\end{aligned}
\tag{12}
$$

The computation of the elastic constants C_{ij} depends on which assumption of ϵ_{zz} we consider. If $\epsilon_{zz}=0$, then C_{ij} are the plane-stress reduced elastic constants:

$$
C_{11}=\frac{E}{1-\nu^2};\quad C_{12}=\nu\frac{E}{1-\nu^2};\quad C_{44}=G;\quad C_{33}=0 \tag{13}
$$

where E is the modulus of elasticity, ν is the Poisson's ratio, and G is the shear modulus $G=\frac{E}{2(1+\nu)}$.

If $\epsilon_{zz}\neq 0$ (thickness stretching), then the elastic coefficients C_{ij} are those of the three-dimensional stress state, given by

$$
C_{11}=\frac{E(1-\nu^2)}{1-3\nu^2-2\nu^3},\quad C_{12}=\frac{E(\nu+\nu^2)}{1-3\nu^2-2\nu^3} \tag{14}
$$

$$
C_{44}=G,\quad C_{33}=\frac{E(1-\nu^2)}{1-3\nu^2-2\nu^3} \tag{15}
$$

3.4 Governing equations and boundary conditions

The governing equations of present theory are derived from the dynamic version of the Principle of Virtual Displacements. The internal virtual work is

$$
\begin{aligned}
\delta U=\int_{\Omega_0}\Bigg\{\int_{-h/2}^{h/2}\Bigg[&\sigma_{xx}\left(\delta\epsilon_{xx}^{(0)}+z\delta\epsilon_{xx}^{(1)}+\sinh\left(\frac{\pi z}{h}\right)\delta\epsilon_{xx}^{(Z)}\right)+\sigma_{yy}\left(\delta\epsilon_{yy}^{(0)}+z\delta\epsilon_{yy}^{(1)}+\sinh\left(\frac{\pi z}{h}\right)\delta\epsilon_{yy}^{(Z)}\right)\\
&+\sigma_{xy}\left(\delta\gamma_{xy}^{(0)}+z\delta\gamma_{xy}^{(1)}+\sinh\left(\frac{\pi z}{h}\right)\delta\gamma_{xy}^{(Z)}\right)+\sigma_{xz}\left(\delta\gamma_{xz}^{(0)}+z\delta\gamma_{xz}^{(1)}+z^2\delta\gamma_{xz}^{(2)}+\frac{\pi}{h}\cosh\left(\frac{\pi z}{h}\right)\delta\gamma_{xz}^{(Z)}\right)\\
&+\sigma_{yz}\left(\delta\gamma_{yz}^{(0)}+z\delta\gamma_{yz}^{(1)}+z^2\delta\gamma_{yz}^{(2)}+\frac{\pi}{h}\cosh\left(\frac{\pi z}{h}\right)\delta\gamma_{yz}^{(Z)}\right)+\sigma_{zz}\left(\delta\epsilon_{zz}^{(0)}+z\delta\epsilon_{zz}^{(1)}\right)\Bigg]dz\Bigg\}dx\,dy
\end{aligned}
\tag{16}
$$

$$\delta U = \int\limits_{\Omega_0} \big(N_{xx}\delta\epsilon_{xx}^{(0)} + M_{xx}\delta\epsilon_{xx}^{(1)} + R_{xx}^{Z}\delta\epsilon_{xx}^{(Z)} + N_{yy}\delta\epsilon_{yy}^{(0)} + M_{yy}\delta\epsilon_{yy}^{(1)} + R_{yy}^{Z}\delta\epsilon_{yy}^{(Z)}$$
$$+ N_{xy}\delta\gamma_{xy}^{(0)} + M_{xy}\delta\gamma_{xy}^{(1)} + R_{xy}^{Z}\delta\gamma_{xy}^{(Z)} + Q_{xz}\delta\gamma_{xz}^{(0)} + M_{xz}\delta\gamma_{xz}^{(1)} + R_{xz}^{2}\delta\gamma_{xz}^{(2)} + R_{xz}^{Z}\delta\gamma_{xz}^{(Z)}$$
$$+ Q_{yz}\delta\gamma_{yz}^{(0)} + M_{yz}\delta\gamma_{yz}^{(1)} + R_{yz}^{2}\delta\gamma_{yz}^{(2)} + R_{yz}^{Z}\delta\gamma_{yz}^{(Z)} + Q_{zz}\delta\epsilon_{zz}^{(0)} + M_{zz}\delta\epsilon_{zz}^{(1)} \big) dx\, dy \tag{17}$$

where Ω_0 is the integration domain on plane (x, y) and

$$\left\{ \begin{array}{c} N_{xx} \\ N_{yy} \\ N_{xy} \end{array} \right\} = \int\limits_{-h/2}^{h/2} \left\{ \begin{array}{c} \sigma_{xx} \\ \sigma_{yy} \\ \sigma_{xy} \end{array} \right\} dz, \quad \left\{ \begin{array}{c} Q_{xz} \\ Q_{yz} \\ Q_{zz} \end{array} \right\} = \int\limits_{-h/2}^{h/2} \left\{ \begin{array}{c} \sigma_{xz} \\ \sigma_{yz} \\ \sigma_{zz} \end{array} \right\} dz \tag{18}$$

$$\left\{ \begin{array}{c} M_{xx} \\ M_{yy} \\ M_{xy} \end{array} \right\} = \int\limits_{-h/2}^{h/2} z \left\{ \begin{array}{c} \sigma_{xx} \\ \sigma_{yy} \\ \sigma_{xy} \end{array} \right\} dz, \quad \left\{ \begin{array}{c} M_{xz} \\ M_{yz} \\ M_{zz} \end{array} \right\} = \int\limits_{-h/2}^{h/2} z \left\{ \begin{array}{c} \sigma_{xz} \\ \sigma_{yz} \\ \sigma_{zz} \end{array} \right\} dz \tag{19}$$

$$\left\{ \begin{array}{c} R_{xx}^{Z} \\ R_{yy}^{Z} \\ R_{xy}^{Z} \end{array} \right\} = \int\limits_{-h/2}^{h/2} \sinh\left(\frac{\pi z}{h}\right) \left\{ \begin{array}{c} \sigma_{xx} \\ \sigma_{yy} \\ \sigma_{xy} \end{array} \right\} dz, \quad \left\{ \begin{array}{c} R_{xz}^{Z} \\ R_{yz}^{Z} \end{array} \right\} = \int\limits_{-h/2}^{h/2} \frac{\pi}{h} \cosh\left(\frac{\pi z}{h}\right) \left\{ \begin{array}{c} \sigma_{xz} \\ \sigma_{yz} \end{array} \right\} dz \tag{20}$$

$$\left\{ \begin{array}{c} R_{xz}^{2} \\ R_{yz}^{2} \end{array} \right\} = \int\limits_{-h/2}^{h/2} z^2 \left\{ \begin{array}{c} \sigma_{xz} \\ \sigma_{yz} \end{array} \right\} dz. \tag{21}$$

The external virtual work due to external loads applied to the plate is given as:

$$\delta V = -\int\limits_{\Omega_0} \left(p_x \delta u + p_y \delta v + p_z \delta w \right) dx\, dy$$
$$= -\int\limits_{\Omega_0} \Big(p_x \left(\delta u_0 + z\delta u_1 + \sinh\left(\frac{\pi z}{h}\right) \delta u_Z \right) + p_y \left(\delta v_0 + z\delta v_1 + \sinh\left(\frac{\pi z}{h}\right) \delta v_Z \right)$$
$$+ p_z \left(\delta w_0 + z\delta w_1 + z^2 \delta w_2 \right) \Big) dx\, dy \tag{22}$$

The external virtual work due to in-plane forces and shear forces applied to the plate is given as:

$$\delta V = -\int\limits_{\Omega_0} \left[\bar{N}_{xx} \frac{\partial w_0}{\partial x} \frac{\delta\partial w_0}{\partial x} + \bar{N}_{xy} \frac{\partial w_0}{\partial y} \frac{\delta\partial w_0}{\partial x} + \bar{N}_{yx} \frac{\partial w_0}{\partial x} \frac{\delta\partial w_0}{\partial y} + \bar{N}_{yy} \frac{\partial w_0}{\partial y} \frac{\delta\partial w_0}{\partial y} \right] dx\, dy \tag{23}$$

being $\bar{N}_{xx}$ and $\bar{N}_{yy}$ the in-plane loads perpendicular to the edges $x = 0$ and $y = 0$ respectively, and $\bar{N}_{xy}$ and $\bar{N}_{yx}$ the distributed shear forces parallel to the edges $x = 0$ and $y = 0$ respectively.

The virtual kinetic energy is given as:

$$
\begin{aligned}
\delta K =& \int_{\Omega_0} \left\{ \int_{-h/2}^{h/2} \rho \left(\dot{u}\delta\dot{u} + \dot{v}\delta\dot{v} + \dot{w}\delta\dot{w} \right) dz \right\} dx\ dy \\
=& \int_{\Omega_0} \big[I_0 \left(\dot{u}_0\delta\dot{u}_0 + \dot{v}_0\delta\dot{v}_0 + \dot{w}_0\delta\dot{w}_0 \right) \\
&+ I_1 \left(\dot{u}_0\delta\dot{u}_1 + \dot{u}_1\delta\dot{u}_0 + \dot{v}_0\delta\dot{v}_1 + \dot{v}_1\delta\dot{v}_0 + \dot{w}_0\delta\dot{w}_1 + \dot{w}_1\delta\dot{w}_0 \right) \\
&+ I_2 \left(\dot{u}_1\delta\dot{u}_1 + \dot{v}_1\delta\dot{v}_1 + \dot{w}_0\delta\dot{w}_2 + \dot{w}_1\delta\dot{w}_1 + \dot{w}_2\delta\dot{w}_0 \right) \\
&+ I_3 \left(\dot{w}_1\delta\dot{w}_2 + \dot{w}_2\delta\dot{w}_1 \right) + I_4\dot{w}_2\delta\dot{w}_2 \\
&+ I_5 \left(\dot{u}_0\delta\dot{u}_Z + \dot{u}_Z\delta\dot{u}_0 + \dot{v}_0\delta\dot{v}_Z + \dot{v}_Z\delta\dot{v}_0 \right) \\
&+ I_6 \left(\dot{u}_Z\delta\dot{u}_Z + \dot{v}_Z\delta\dot{v}_Z \right) \\
&+ I_7 \left(\dot{u}_1\delta\dot{u}_Z + \dot{u}_Z\delta\dot{u}_1 + \dot{v}_Z\delta\dot{v}_1 + \dot{v}_1\delta\dot{v}_Z \right) \big] dx\ dy
\end{aligned}
\tag{24}
$$

where the dots denote the derivative with respect to time t and the inertia terms are defined as

$$
I_i = \int_{-h/2}^{h/2} \rho z^i dz \quad i = 0, 1, 2, 3, 4 \tag{25}
$$

$$
I_5 = \int_{-h/2}^{h/2} \rho \sinh\left(\frac{\pi z}{h}\right) dz; \quad I_6 = \int_{-h/2}^{h/2} \rho \sinh^2\left(\frac{\pi z}{h}\right) dz; \quad I_7 = \int_{-h/2}^{h/2} \rho z \sinh\left(\frac{\pi z}{h}\right) dz \tag{26}
$$

Substituting δU, δV, and δK in the virtual work statement, integrating by parts with respect to x, y, and t and collecting the coefficients of δu_0, δu_1, δu_Z, δv_0, δv_1, δv_Z,

δw_0, δw_1, δw_2, the following governing equations are obtained:

$$\delta u_0: -\frac{\partial N_{xx}}{\partial x} - \frac{\partial N_{xy}}{\partial y} = \int_{-h/2}^{h/2} \left\{\rho\left(\ddot{u}_0 + z\ddot{u}_1 + \sinh\left(\frac{\pi z}{h}\right)\ddot{u}_Z\right) + p_x\right\} dz$$

$$\delta v_0: -\frac{\partial N_{xy}}{\partial x} - \frac{\partial N_{yy}}{\partial y} = \int_{-h/2}^{h/2} \left\{\rho\left(\ddot{v}_0 + z\ddot{v}_1 + \sinh\left(\frac{\pi z}{h}\right)\ddot{v}_Z\right) + p_y\right\} dz$$

$$\delta w_0: -\frac{\partial Q_{xz}}{\partial x} - \frac{\partial Q_{yz}}{\partial y} + \bar{N}_{xx}\frac{\partial^2 w_0}{\partial x^2} + \bar{N}_{xy}\frac{\partial^2 w_0}{\partial y \partial x} + \bar{N}_{yx}\frac{\partial^2 w_0}{\partial x \partial y}$$
$$+ \bar{N}_{yy}\frac{\partial^2 w_0}{\partial y^2} = \int_{-h/2}^{h/2} \left\{\rho\left(\ddot{w}_0 + z\ddot{w}_1 + z^2\ddot{w}_2\right) + p_z\right\} dz$$

$$\delta u_1: -\frac{\partial M_{xx}}{\partial x} - \frac{\partial M_{xy}}{\partial y} + Q_{xz} = \int_{-h/2}^{h/2} \left\{\rho z\left(\ddot{u}_0 + z\ddot{u}_1 + \sinh\left(\frac{\pi z}{h}\right)\ddot{u}_Z\right) + zp_x\right\} dz$$

$$\delta v_1: -\frac{\partial M_{xy}}{\partial x} - \frac{\partial M_{yy}}{\partial y} + Q_{yz} = \int_{-h/2}^{h/2} \left\{\rho z\left(\ddot{v}_0 + z\ddot{v}_1 + \sinh\left(\frac{\pi z}{h}\right)\ddot{v}_Z\right) + zp_y\right\} dz$$

$$\delta w_1: -\frac{\partial M_{xz}}{\partial x} - \frac{\partial M_{yz}}{\partial y} + Q_{zz} = \int_{-h/2}^{h/2} \left\{\rho z\left(\ddot{w}_0 + z\ddot{w}_1 + z^2\ddot{w}_2\right) + zp_z\right\} dz$$

$$\delta u_Z: -\frac{\partial R^Z_{xx}}{\partial x} - \frac{\partial R^Z_{xy}}{\partial y} + R^Z_{xz} = \int_{-h/2}^{h/2} \left\{\rho\sinh\left(\frac{\pi z}{h}\right)\left(\ddot{u}_0 + z\ddot{u}_1 + \sinh\left(\frac{\pi z}{h}\right)\ddot{u}_Z\right) + \sinh\left(\frac{\pi z}{h}\right)p_x\right\} dz$$

$$\delta v_Z: -\frac{\partial R^Z_{xy}}{\partial x} - \frac{\partial R^Z_{yy}}{\partial y} + R^Z_{yz} = \int_{-h/2}^{h/2} \left\{\rho\sinh\left(\frac{\pi z}{h}\right)\left(\ddot{v}_0 + z\ddot{v}_1 + \sinh\left(\frac{\pi z}{h}\right)\ddot{v}_Z\right) + \sinh\left(\frac{\pi z}{h}\right)p_y\right\} dz$$

$$\delta w_2: -\frac{\partial R^2_{xz}}{\partial x} - \frac{\partial R^2_{yz}}{\partial y} + 2M_{zz} = \int_{-h/2}^{h/2} \left\{\rho z^2\left(\ddot{w}_0 + z\ddot{w}_1 + z^2\ddot{w}_2\right) + z^2p_z\right\} dz \tag{27}$$

The mechanical boundary conditions are:

grid	13^2	17^2	21^2
$\bar{P}$	4.05112	4.05070	4.05065

Table 1: Convergence study for the uni-axial buckling load of a simply supported 2-2-1 sandwich square plate with FGM skins and $p = 5$ case using the higher-order theory.

$$\begin{aligned}
\delta u_0 &: n_x N_{xx} + n_y N_{xy} = n_x \bar{N}_{xx} + n_y \bar{N}_{xy} \\
\delta v_0 &: n_x N_{xy} + n_y N_{yy} = n_x \bar{N}_{xy} + n_y \bar{N}_{yy} \\
\delta w_0 &: n_x Q_{xz} + n_y Q_{yz} = n_x \bar{Q}_{xz} + n_y \bar{Q}_{yz} \\
\delta u_1 &: n_x M_{xx} + n_y M_{xy} = n_x \bar{M}_{xx} + n_y \bar{M}_{xy} \\
\delta v_1 &: n_x M_{xy} + n_y M_{yy} = n_x \bar{M}_{xy} + n_y \bar{M}_{yy} \\
\delta w_1 &: n_x M_{xz} + n_y M_{yz} = n_x \bar{M}_{xz} + n_y \bar{M}_{yz} \\
\delta u_Z &: n_x R^Z_{xx} + n_y R^Z_{xy} = n_x \bar{R}^Z_{xx} + n_y \bar{R}^Z_{xy} \\
\delta v_Z &: n_x R^Z_{xy} + n_y R^Z_{yy} = n_x \bar{R}^Z_{xy} + n_y \bar{R}^Z_{yy} \\
\delta w_2 &: n_x R^2_{xz} + n_y R^2_{yz} = n_x \bar{R}^2_{xz} + n_y \bar{R}^2_{yz}
\end{aligned} \tag{28}$$

where (n_x, n_y) denotes the unit normal-to-boundary vector.

4 Numerical examples

The higher-order plate theory and collocation with RBFs are considered for the uni-axial and bi-axial buckling analysis of simply supported functionally graded sandwich square plates ($a = b$) of type C with side-to-thickness ratio $a/h = 10$.

The material properties considered are $E_m = 70E_0$ (aluminum) for the metal and $E_c = 380E_0$ (alumina) for the ceramic being $E_0 = 1$GPa. The non-dimensional parameter used is

$$\bar{P} = \frac{Pa^2}{100h^3E_0}.$$

An initial convergence study with the higher-order theory was conducted for each buckling load type using 13^2, 17^2, and 21^2 grids. In table 1 the uniaxial case is shown for the 2-2-1 sandwich with $p = 5$ and in table 2 the bi-axial case is presented for the 1-2-1 sandwich with $p = 1$. In the following, results are obtained by considering a grid of 17^2 points, which seems acceptable by the convergence study.

In tables 3 and 4 the critical buckling loads obtained from the present approach with $\epsilon_{zz} \neq 0$ and $\epsilon_{zz} = 0$ are tabulated for various power-law exponents p and thickness ratios. Both tables include results obtained from classical plate theory (CLPT), first-order shear deformation plate theory (FSDPT, $K = 5/6$ as shear correction factor), Reddy's higher-order shear deformation plate theory (TSDPT) [16], and Zenkour's

grid	13^2	17^2	21^2
$\bar{P}$	3.66028	3.65998	3.65994

Table 2: Convergence study for the bi-axial buckling load of a simply supported 1-2-1 sandwich square plate with FGM skins and $p = 1$ case using the higher-order theory.

sinusoidal shear deformation plate theory (SSDPT) [5]. Table 3 refers to the uni-axial buckling load and table 4 refers to the bi-axial buckling load.

A good agreement between the present solution and references considered, specially [16] and [5] is obtained. This allow us to conclude that the present higher-order plate theory is good for the modeling of simply supported sandwich FGM plates and that collocation with RBFs is a good formulation. Present results with $\epsilon_{zz} = 0$ approximates better references [16] and [5] than $\epsilon_{zz} \neq 0$ as the authors use the $\epsilon_{zz} = 0$ approach. This study also lead us to conclude that the thickness stretching effect has a strong influence on the buckling analysis of sandwich FGM plates as $\epsilon_{zz} = 0$ gives higher fundamental buckling loads than $\epsilon_{zz} \neq 0$.

The isotropic fully ceramic plate (first line on tables 3 and 4) has the higher fundamental buckling loads. As the core thickness to the total thickness of the plate ratio $((h_2 - h_1)/h)$ increases the buckling loads increase as well. We may conclude that the critical buckling loads decrease as the power-law exponent p increases. By comparing tables 3 and 4 we also conclude that the bi-axial buckling load of simply supported sandwich square plate with FGM skins is half the uni-axial one for the same plate.

In figure 4 the first four buckling modes of a simply supported 2-1-2 sandwich square plate with FGM skins, $p = 0.5$, subjected to a uni-axial in-plane compressive load, using the higher-order plate theory and 17^2 grid is presented. Figure 5 presents the first four buckling modes of a simply supported 2-1-1 sandwich square plate with FGM skins, $p = 10$, subjected to a bi-axial in-plane compressive load.

5 Conclusions

An application of a Unified formulation by a meshless discretization is proposed, based on a thickness-stretching hyperbolic sine shear deformation theory that was implemented for the buckling analysis of functionally graded sandwich plates.

The present formulation was compared with analytical, meshless or finite element methods and showed very accurate results. The effect of $\epsilon_{zz} \neq 0$ showed to be significant in such sandwich problems.

Acknowledgments

Ana M. A. Neves acknowledges support from FCT grant SFRH/BD/45554/2008.

		$\bar{P}$					
p	Theory	1-0-1	2-1-2	2-1-1	1-1-1	2-2-1	1-2-1
0	CLPT	13.73791	13.73791	13.73791	13.73791	13.73791	13.73791
	FSDPT	13.00449	13.00449	13.00449	13.00449	13.00449	13.00449
	TSDPT [16]	13.00495	13.00495	13.00495	13.00495	13.00495	13.00495
	SSDPT [5]	13.00606	13.00606	13.00606	13.00606	13.00606	13.00606
	present $\epsilon_{zz} \neq 0$	12.95287	12.95287	12.95287	12.95287	12.95287	12.95287
	present $\epsilon_{zz} = 0$	13.00508	13.00508	13.00508	13.00508	13.00508	13.00508
0.5	CLPT	7.65398	8.25597	8.56223	8.78063	9.18254	9.61525
	FSDPT	7.33732	7.91320	8.20015	8.41034	8.78673	9.19517
	TSDPT [16]	7.36437	7.94084	8.22470	8.43645	8.80997	9.21681
	SSDPT [5]	7.36568	7.94195	8.22538	8.43712	8.81037	9.21670
	present $\epsilon_{zz} \neq 0$	7.16207	7.71627	7.98956	8.19278	8.55172	8.94190
	present $\epsilon_{zz} = 0$	7.18728	7.74326	8.01701	8.22133	8.58129	8.97310
1	CLPT	5.33248	6.02733	6.40391	6.68150	7.19663	7.78406
	FSDPT	5.14236	5.81379	6.17020	6.43892	6.92571	7.48365
	TSDPT [16]	5.16713	5.84006	6.19394	6.46474	6.94944	7.50656
	SSDPT [5]	5.16846	5.84119	6.19461	6.46539	6.94980	7.50629
	present $\epsilon_{zz} \neq 0$	5.06137	5.71135	6.05467	6.31500	6.78405	7.31995
	present $\epsilon_{zz} = 0$	5.07848	5.73022	6.07358	6.33556	6.80547	7.34367
5	CLPT	2.73080	3.10704	3.48418	3.65732	4.21238	4.85717
	FSDPT	2.63842	3.02252	3.38538	3.55958	4.09285	4.71475
	TSDPT [16]	2.65821	3.04257	3.40351	3.57956	4.11209	4.73469
	SSDPT [5]	2.66006	3.04406	3.40449	3.58063	4.11288	4.73488
	present $\epsilon_{zz} \neq 0$	2.63652	3.00791	3.36255	3.53005	4.05070	4.64701
	present $\epsilon_{zz} = 0$	2.64681	3.01865	3.37196	3.54148	4.06163	4.66059
10	CLPT	2.56985	2.80340	3.16427	3.25924	3.79238	4.38221
	FSDPT	2.46904	2.72626	3.07428	3.17521	3.68890	4.26040
	TSDPT [16]	2.48727	2.74632	3.09190	3.19471	3.70752	4.27991
	SSDPT [5]	2.48928	2.74844	3.13443	3.19456	3.14574	4.38175
	present $\epsilon_{zz} \neq 0$	2.47216	2.72046	3.06067	3.15761	3.66166	4.20550
	present $\epsilon_{zz} = 0$	2.48219	2.73080	3.06943	3.16837	3.67153	4.21792

Table 3: Uni-axial buckling load of simply supported plate of C-type using the higher-order theory and a grid with 17^2 points.

p	Theory	$\bar{P}$ 1-0-1	2-1-2	2-1-1	1-1-1	2-2-1	1-2-1
0	CLPT	6.86896	6.86896	6.86896	6.86896	6.86896	6.86896
	FSDPT	6.50224	6.50224	6.50224	6.50224	6.50224	6.50224
	TSDPT [16]	6.50248	6.50248	6.50248	6.50248	6.50248	6.50248
	SSDPT [5]	6.50303	6.50303	6.50303	6.50303	6.50303	6.50303
	present $\epsilon_{zz} \neq 0$	6.47643	6.47643	6.47643	6.47643	6.47643	6.47643
	present $\epsilon_{zz} = 0$	6.50254	6.50254	6.50254	6.50254	6.50254	6.50254
0.5	CLPT	3.82699	4.12798	4.28112	4.39032	4.59127	4.80762
	FSDPT	3.66866	3.95660	4.10007	4.20517	4.39336	4.59758
	TSDPT [16]	3.68219	3.97042	4.11235	4.21823	4.40499	4.60841
	SSDPT [5]	3.68284	3.97097	4.11269	4.21856	4.40519	4.60835
	present $\epsilon_{zz} \neq 0$	3.58104	3.85813	3.99478	4.09639	4.27586	4.47095
	present $\epsilon_{zz} = 0$	3.59364	3.87163	4.00851	4.11067	4.29064	4.48655
1	CLPT	2.66624	3.01366	3.20195	3.34075	3.59831	3.89203
	FSDPT	2.57118	2.90690	3.08510	3.21946	3.46286	3.74182
	TSDPT [16]	2.58357	2.92003	3.09697	3.23237	3.47472	3.75328
	SSDPT [5]	2.58423	2.92060	3.09731	3.23270	3.47490	3.75314
	present $\epsilon_{zz} \neq 0$	2.53069	2.85568	3.02733	3.15750	3.39202	3.65998
	present $\epsilon_{zz} = 0$	2.53924	2.86511	3.03679	3.16778	3.40274	3.67183
5	CLPT	1.36540	1.55352	1.74209	1.82866	2.10619	2.42859
	FSDPT	1.31921	1.51126	1.69269	1.77979	2.04642	2.35737
	TSDPT [16]	1.32910	1.52129	1.70176	1.78978	2.05605	2.36734
	SSDPT [5]	1.33003	1.52203	1.70224	1.79032	2.05644	2.36744
	present $\epsilon_{zz} \neq 0$	1.31826	1.50395	1.68128	1.76502	2.02535	2.32351
	present $\epsilon_{zz} = 0$	1.32340	1.50933	1.68598	1.77074	2.03081	2.33029
10	CLPT	1.28493	1.40170	1.58214	1.62962	1.89619	2.19111
	FSDPT	1.23452	1.36313	1.53714	1.58760	1.84445	2.13020
	TSDPT [16]	1.24363	1.37316	1.54595	1.59736	1.85376	2.13995
	SSDPT [5]	1.24475	1.37422	1.56721	1.59728	1.57287	2.19087
	present $\epsilon_{zz} \neq 0$	1.23608	1.36023	1.53034	1.57880	1.83083	2.10275
	present $\epsilon_{zz} = 0$	1.24109	1.36540	1.53472	1.58419	1.83576	2.10896

Table 4: Bi-axial buckling load of simply supported plate of C-type using the higher-order theory and a grid with 17^2 points.

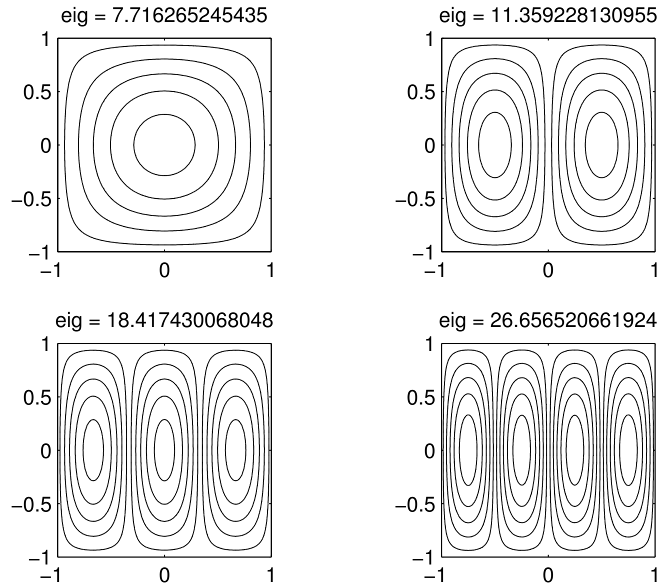

Figure 4: First four buckling modes. Uni-axial buckling load of a simply supported 2-1-2 plate C-type, $p = 0.5$, a 17^2 points grid, and using the higher-order theory.

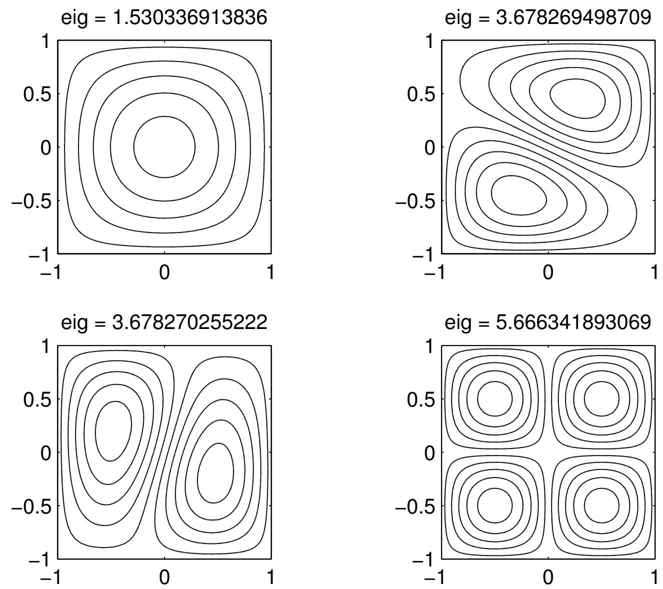

Figure 5: First four buckling modes. Bi-axial buckling load of a simply supported 2-1-1 plate C-type, $p = 10$, a 17^2 points grid, and using the higher-order theory.

References

[1] Y. Miyamoto, W.A. Kaysser, B.H. Rabin, A. Kawasaki, and R.G. Ford. *Functionally Graded Materials: Design, Processing and Applications*. Kluwer Academic Publishers, 1999.

[2] R.C. Batra and J. Jin. Natural frequencies of a functionally graded anisotropic rectangular plate. *Journal of Sound and Vibration*, 282(1-2):509 – 516, 2005.

[3] A. J. M. Ferreira, R. C. Batra, C. M. C. Roque, L. F. Qian, and R. M. N. Jorge. Natural frequencies of functionally graded plates by a meshless method. *Composite Structures*, 75(1-4):593–600, September 2006.

[4] S. S. Vel and R. C. Batra. Three-dimensional exact solution for the vibration of functionally graded rectangular plates. *Journal of Sound and Vibration*, 272:703–730, 2004.

[5] A.M. Zenkour. A comprehensive analysis of functionally graded sandwich plates: Part 2–buckling and free vibration. *International Journal of Solids and Structures*, 42(18-19):5243 – 5258, 2005.

[6] Z. Q. Cheng and R. C. Batra. Exact correspondence between eigenvalues of membranes and functionally graded simply supported polygonal plates. *Journal of Sound and Vibration*, 229:879–895, 2000.

[7] M. M. Najafizadeh and M. R. Eslami. Buckling analysis of circular plates of functionally graded materials under uniform radial compression. *International Journal of Mechanical Sciences*, 44(12):2479 – 2493, 2002.

[8] V. Birman. Buckling of functionally graded hybrid composite plates. *Proceedings of the 10th Conference on Engineering Mechanics*, pages 1199–1202, 1995.

[9] R. Javaheri and M.R. Eslami. Buckling of functionally graded plates under inplane compressive loading. *ZAMM - Journal of Applied Mathematics and Mechanics / Zeitschrift fr Angewandte Mathematik und Mechanik*, 82(4):277–283, 2002.

[10] Shyang-Ho Chi and Yen-Ling Chung. Mechanical behavior of functionally graded material plates under transverse load–part i: Analysis. *International Journal of Solids and Structures*, 43(13):3657 – 3674, 2006.

[11] Shyang-Ho Chi and Yen-Ling Chung. Mechanical behavior of functionally graded material plates under transverse load–part ii: Numerical results. *International Journal of Solids and Structures*, 43(13):3675 – 3691, 2006.

[12] A. M. Zenkour. Generalized shear deformation theory for bending analysis of functionally graded plates. *Appl Math Modell*, 30:67–84, 2006.

[13] Z. Q. Cheng and R. C. Batra. Deflection relationships between the homogeneous kirchhoff plate theory and different functionally graded plate theories. *Archive of Mechanics*, 52:143–158, 2000.

[14] L. F. Qian, R. C. Batra, and L. M. Chen. Static and dynamic deformations of thick functionally graded elastic plate by using higher-order shear and normal deformable plate theory and meshless local petrov-galerkin method. *Composites: Part B*, 35:685–697, 2004.

[15] A. J. M. Ferreira, R. C. Batra, C. M. C. Roque, L. F. Qian, and P. A. L. S. Martins.

Static analysis of functionally graded plates using third-order shear deformation theory and a meshless method. *Composite Structures*, 69(4):449–457, 2005.

[16] J. N. Reddy. Analysis of functionally graded plates. *International Journal for Numerical Methods in Engineering*, 47:663–684, 2000.

[17] E. Carrera. C^0 reissner-mindlin multilayered plate elements including zig-zag and interlaminar stress continuity. *International Journal of Numerical Methods in Engineering*, 39:1797–1820, 1996.

[18] E. Carrera. Developments, ideas, and evaluations based upon reissner's mixed variational theorem in the modelling of multilayered plates and shells. *Applied Mechanics Reviews*, 54:301–329, 2001.

[19] E. J. Kansa. Multiquadrics- a scattered data approximation scheme with applications to computational fluid dynamics. i: Surface approximations and partial derivative estimates. *Computers and Mathematics with Applications*, 19(8/9):127–145, 1990.

[20] A. J. M. Ferreira. A formulation of the multiquadric radial basis function method for the analysis of laminated composite plates. *Composite Structures*, 59:385–392, 2003.

[21] A. J. M. Ferreira. Thick composite beam analysis using a global meshless approximation based on radial basis functions. *Mechanics of Advanced Materials and Structures*, 10:271–284, 2003.

[22] A. J. M. Ferreira, C. M. C. Roque, and P. A. L. S. Martins. Analysis of composite plates using higher-order shear deformation theory and a finite point formulation based on the multiquadric radial basis function method. *Composites: Part B*, 34:627–636, 2003.

[23] A.J.M. Ferreira, C.M.C. Roque, R.M.N. Jorge, and E.J. Kansa. Static deformations and vibration analysis of composite and sandwich plates using a layerwise theory and multiquadrics discretizations. *Engineering Analysis with Boundary Elements*, 29(12):1104 – 1114, 2005.

[24] A.J.M. Ferreira, C.M.C. Roque, and R.M.N. Jorge. Analysis of composite plates by trigonometric shear deformation theory and multiquadrics. *Computers & Structures*, 83(27):2225 – 2237, 2005.

[25] A.J.M. Ferreira, R.C. Batra, C.M.C. Roque, L.F. Qian, and R.M.N. Jorge. Natural frequencies of functionally graded plates by a meshless method. *Composite Structures*, 75(1-4):593 – 600, 2006. Thirteenth International Conference on Composite Structures - ICCS/13.

[26] A.J.M. Ferreira, C.M.C. Roque, and R.M.N. Jorge. Free vibration analysis of symmetric laminated composite plates by fsdt and radial basis functions. *Computer Methods in Applied Mechanics and Engineering*, 194(39-41):4265 – 4278, 2005.

[27] A. J. M. Ferreira, C. M. C. Roque, and P. A. L. S. Martins. Radial basis functions and higher-order shear deformation theories in the analysis of laminated composite beams and plates. *Composite Structures*, 66(1-4):287 – 293, 2004. Twelfth International Conference on Composite Structures.

[28] A.M.A. Neves, A.J.M. Ferreira, E. Carrera, C.M.C. Roque, M. Cinefra, R. M.N.

Jorge, and C.M.M. Soares. Bending of fgm plates by a sinusoidal plate formulation and collocation with radial basis functions. *Mechanics Research Communications*, In Press, Accepted Manuscript:–, 2011.

[29] A.M.A. Neves, A.J.M. Ferreira, E. Carrera, C.M.C. Roque, M. Cinefra, R. M.N. Jorge, and C.M.M. Soares. A quasi-3d sinusoidal shear deformation theory for the static and free vibration analysis of functionally graded plates. *Composites Part B*, In Press, Accepted Manuscript:–, 2011.